J Comput Aided Mol Des (2012) 26:329–337
DOI 10.1007/s10822-012-9559-9

Understanding the mechanism of cellulose dissolution in 1-butyl-3-methylimidazolium chloride ionic liquid via quantum chemistry calculations and molecular dynamics simulations

Hao Xu · Wenxiao Pan · Ruoxi Wang · Dongju Zhang · Chengbu Liu

Received: 13 October 2011 / Accepted: 1 March 2012 / Published online: 16 March 2012

Abstract While *N,N′*-dialkylimidazolium ionic liquids (ILs) have been well-established as effective solvents for dissolution and processing of cellulose, the detailed mechanism at the molecular level still remains unclear. In this work, we present a combined quantum chemistry and molecular dynamics simulation study on how the ILs dissolve cellulose. On the basis of calculations on 1-butyl-3-methylimidazolium chloride, one of the most effective ILs dissolving cellulose, we further studied the molecular behavior of cellulose models (i.e. cellulose oligomers with degrees of polymerization $n = 2$, 4, and 6) in the IL, including the structural features and hydrogen bonding patterns. The collected data indicate that both chloride anions and imidazolium cations of the IL interact with the oligomer via hydrogen bonds. However, the anions occupy the first coordination shell of the oligomer, and the strength and number of hydrogen bonds and the interaction energy between anions and the oligomer are much larger than those between cations and the oligomer. It is observed that the intramolecular hydrogen bond in the oligomer is broken under the combined effect of anions and cations. The present results emphasize that the chloride anions play a critically important role and the imidazolium cations also present a remarkable contribution in the cellulose dissolution. This point of view is different from previous one that only underlines the importance of the chloride anions in the cellulose dissolution. The present results improve our understanding for the cellulose dissolution in imidazolium chloride ILs.

Keywords Cellulose · Ionic liquids · 1-Butyl-3-methylimidazolium chloride · Quantum chemistry · Molecular dynamics

Introduction

With the decreasing fossil fuel resources and the increasing environmental pollution problems, it is an inevitable trend to find new kinds of alternative energy resources which are renewable and environmentally friendly. The most abundant biorenewable resource in environment is cellulose [1], the major component of plant cell walls. In recent years, cellulose is attracting more and more attention due to its advantages as a cheap and nontoxic raw material to produce numerous useful products [2, 3], and many countries are paying interests to the technology of using cellulose to yield fuel ethanol [4, 5], which could be used as energy resource instead of fossil resources. However, there are still some open issues hindering the utilization of cellulose, in which one principal challenge is its poor solubility in most solvents due to the existence of a huge number of intramolecular and intermolecular hydrogen bonds in cellulose

Electronic supplementary material The online version of this article (doi:10.1007/s10822-012-9559-9) contains supplementary material, which is available to authorized users.

H. Xu · W. Pan · R. Wang · D. Zhang (✉) · C. Liu
Key Laboratory of Colloid and Interface Chemistry, Ministry of Education, Jinan 250100, People's Republic of China
e-mail: zhangdj@sdu.edu.cn

H. Xu · W. Pan · R. Wang · D. Zhang · C. Liu
School of Chemistry and Chemical Engineering, Shandong University, Jinan 250100, People's Republic of China

R. Wang
Criminal Scientific and Technological Department, Shandong Police College, Jinan 250014, People's Republic of China

[6]. Furthermore, there are also many disadvantages of the traditional cellulose solution methods, which usually require relatively harsh conditions and expensive and uncommon solvents with un-environmentally friendly processes [7–10].

Ionic liquids (ILs) are a new class of liquids that are composed of ions completely, and their melting points are generally less than 100 °C. Over the past decades, ILs have caused more and more attention [11–16] due to their remarkable properties [17–20], such as high thermal and chemical stability, negligible vapor pressure, nonflammability, reusability, and designability. In addition, the mixtures of ILs with other organic liquids, such as acetonitrile, have also attracted research interests in recent years [21, 22], and their physical chemical properties have been well studied by Chaban et al. [15, 16] using the atomistic simulation study to provide guidance to the potential technological applications. ILs are generally used as "green solvents" in chemical synthesis and extraction separation processes. Early in 1934, Graenacher [23] had ever reported the dissolution of cellulose in molten *N*-ethylpyridinium chloride IL, but this was regarded as useless in that time. Up to 2002, the finding of Rogers et al. [24] that imidazolium-based ILs could dissolve cellulose really opens a new way for the application of cellulose. After that, many theoretical [25–31] and experimental [32–34] studies have been carried out to understand the mechanism of cellulose dissolution in ILs and to design efficient solvents for cellulose. However, there is still no consistent conclusion of cellulose dissolution mechanism in ILs. For example, via NMR analysis, Remsing et al. [32, 33] proposed that the anions of ILs play a critical role in the cellulose dissolution process, and the interaction of the cations with cellulose is nonspecific. In contrast, Zhang et al. [34] considered that the cations of ILs are mainly responsible for the cellulose dissolution in ILs. So further studies for the interaction between cellulose and ILs should be carried out.

Here, we choose 1-butyl-3-methylimidazolium chloride IL (denoted as [BMIM]Cl) as a representative of imidazolium-based ILs for study because it was proposed to be one of the most efficient cellulose solvents [35, 36]. We present a combined quantum chemistry (QM) and molecular dynamics (MD) simulation study on the complex systems consisting of [BMIM]Cl and the cellulose oligomer to show the mechanism details of the interactions between cellulose and the IL at the molecular level. Cellulose is a polysaccharide formed by the polymerization of a few hundred to over several thousand β-(1,4)-D-glucose units [37, 38], and the repeat unit in cellulose is cellobiose comprised of two glucose units [39, 40]. Cellulose oligomers with degrees of polymerization $n = 2$, 4, and 6 are used as cellulose models.

Computational details

Initial configurations of the oligomers were obtained using the Glycam Biomolecule Builder, a free online builder for carbohydrates and related molecules [41]. Fig. 1S in the electronic supplementary material shows three so-built linear cellulose oligomers containing 2, 4, and 6 glucose units, where there exists an intramolecular hydrogen bond between two neighboring saccharide rings and all the saccharide rings prefer chair conformations. Quantum chemistry calculations of isolated ionic pair [BMIM]Cl and cellulose oligomers were carried out at the B3LYP/6-311+G(d,p) level by using the Gaussian 03 program package [42]. Vibrational frequencies were calculated at the same level in order to check whether the optimized structures correspond to true local minima and to provide zero-point vibrational energies (ZPEs). The optimized structures of isolated ionic pair and cellulose oligomers were then used as building blocks of the MD simulation systems.

For MD simulations, we used AMBER type force field, whose potential function form is [43]:

$$E_{\text{total}} = \sum_{\text{bonds}} K_r(r - r_{\text{eq}})^2 + \sum_{\text{angles}} K_\theta(\theta - \theta_{\text{eq}})^2 + \sum_{\text{dihedrals}} \frac{V_n}{2}[1 + \cos(n\phi - \gamma)] + \sum_{i<j} \left[\frac{Aij}{R_{ij}^{12}} - \frac{Bij}{R_{ij}^{6}} + \frac{q_i q_j}{\varepsilon R_{ij}}\right] \quad (1)$$

where, the first three terms in Eq. (1) describe bonds, angles, and dihedrals interactions, respectively, and the last term is nonbonded interaction, including van der Waals and Coulombic interactions. For [BMIM]Cl, a non-standard solvent, its parameters are not currently part of the AMBER force field. Fortunately, many force field models of ILs have been recently developed to mimic their structural, dynamical, and thermodynamic properties. For instance, for imidazolium-based ILs concerned here, Wang et al. [44] initially developed an all-atom force field in the frame of AMBER, and very recently, this force field was refined by Chaban et al. [45–47] to accurately simulate transport properties of the ILs. In our present work, we borrowed the force field of [BMIM]Cl developed by Wang et al. [44] in view of fact that the parameters of both the cation and anion were optimized based an identical method. For cellulose oligomers, the GLYCAM [48] force field was employed. Such a method using fixed force field parameters is often employed to simulate the interaction of a solute with a non-standard solvent [28, 30]. In particular, in a very recent work, Liu et al. [30] have confirmed the reliability of the combination of AMBER based force field parameters and the GLYCAM force field parameters for

describing the interaction between imidazolium-based ILs and cellulose oligomers.

MD simulations were performed with the GROMACS 4.5.1 [49–52] software package. Leapfrog algorithm was used to integrate the Newton's equations of motion. The time step was 1 fs, and data were collected every 1,000 time steps for analysis. The long-range electrostatic interactions were computed by using the particle mesh Ewald method [53, 54], with the cutoff distance was set to 1.2 nm.

The pure IL system and three cellulose oligomer/IL systems for MD simulations include 256 [BMIM]Cl ionic pairs. The energies of model systems were first minimized using the steepest descent method, and then equilibrated in the NVT ensemble for 3 ns. The final production runs were performed in the NPT ensemble ($P = 1$ bar) for 5 ns after an initial equilibrium of 5 ns. Because the equilibrium state of a system can be reached easily at high temperatures, our simulation on the pure IL system was initially pre-equilibrated at 600 K and then cooled down to the target temperature 373 K (i.e., above the melting point of [BMIM]Cl, ~347 K), at which Rogers et al. [24] carried out their experimental study of the dissolution of cellulose in imidazolium-based ILs. Once the equilibrium state of the pure IL system was reached, we put one cellulose oligomer into solvent box to get the initial configuration of the cellulose oligomer/IL system. In addition, the pre-equilibrated pure IL system at 600 K was also cooled down to 298 K to obtain the liquid density, whose experimental value is available for comparison. The Berendsen thermostat/barostat algorithm [55] was utilized in all MD simulations.

Results and discussion

Structures of an isolated [BMIM]Cl ionic pair and cellulose oligomers

Figure 1 shows the most stable geometries of an isolated ionic pair (panel (a)) and three cellulose oligomers (panels (b), (c), and (d)), optimized at the B3LYP/6-311+G(d,p) level. For the ionic pair, we have considered various possible orientations between anion and cation. As shown by panel (a) in Fig. 1, the ionic pair is the most stable as the chlorine anion occurs in the vicinity of the C2–H bond of the cation. This can be attributed to the larger positive charge on the C2–H unit (0.181 *e*) than on other C–H units, such as 0.123 *e* on the C4–H unit and 0.111 *e* on the C5–H unit. The calculated H···Cl distance is 2.005 Å, which is remarkably shorter than the summation (2.95 Å) of the van der Waals radii of Cl and H atoms [56], and the determined C2–H···Cl angle is 159.2°. These data indicate the formation of C2–H···Cl H-bond between the anion and cation clearly. The energy of formation of the ionic pair is calculated to be 90.35 kcal mol^{-1}. The effective hydrogen bond and the strong Coulomb interaction between the cation and anion are in agreement with the observed high

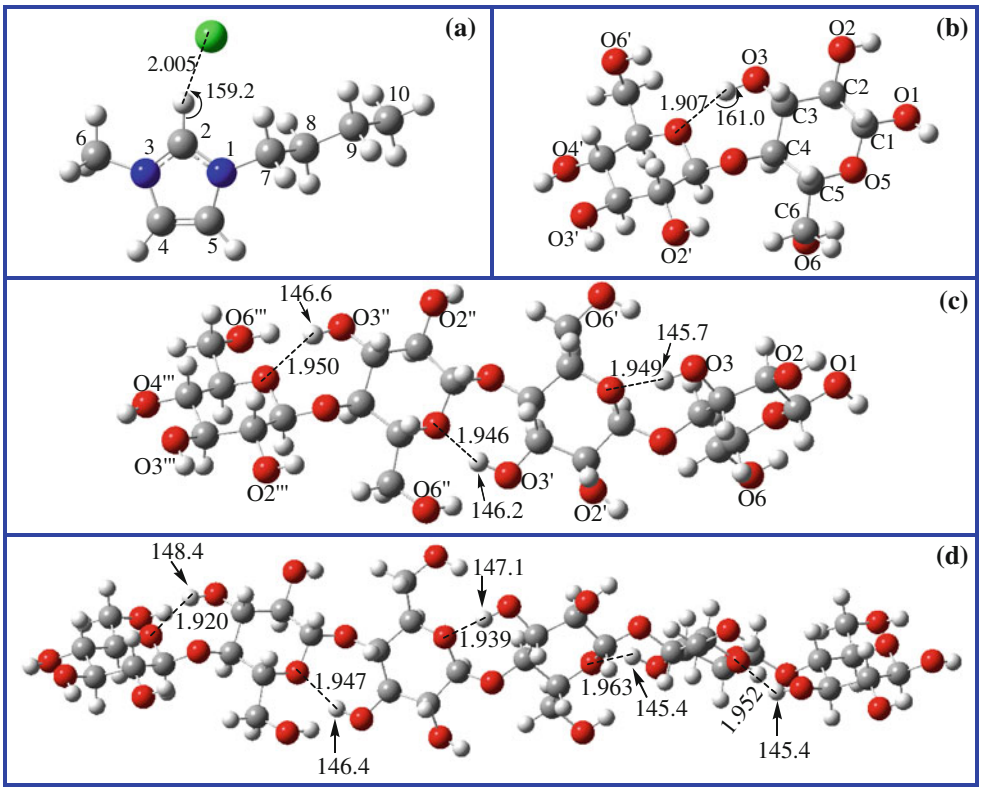

Fig. 1 Optimized geometries at the B3LYP/6-311+G(d,p) level for (**a**) an isolated ion pair [BMIM]Cl, and (**b**), (**c**), and (**d**) for cellulose oligomers with 2, 4, and 6 glucose units respectively. *Bond* distances are shown in Angstrom, and the angles are in degree

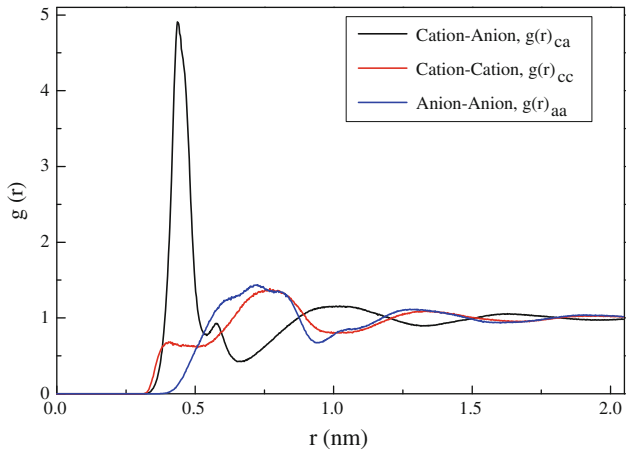

Fig. 2 RDFs of the cation–anion, cation-cation and anion-anion pairs. The geometrical center of the imidazolium ring and the entire Cl atom were taken into account as the positions of the cation and the anion

viscosity, low vapor pressure and good thermal stability of [BMIM]Cl IL [57].

For three cellulose oligomers, structures (b), (c) and (d) shown in Fig. 1, we observe two common features of their geometries: (i) the saccharide rings keep a chair conformation as it is in bulk crystalline cellulose [58, 59], indicating these oligomers are structurally suitable for mimicing a real cellulose chain, and (ii) the ring oxygen (O_{ring}) in a monosaccharide establishes an important hydrogen bridge with the C3 hydroxyl group in the next monosaccharide. As shown in Fig. 1, the hydrogen bond distances vary between 1.9 and 2.0 Å, which are shorter than the summation (2.72 Å) of the van der Waals radii of O and H atoms, and the O–H···O angles are in a range of 140–170°. The parameters of these hydrogen bonds show obviously that there exists strong intramolecular hydrogen bonding interaction in a cellulose chain except the well-known intermolecular H-bonds between cellulose chains. These intramolecular hydrogen bonds are expected to be an important factor resulting in the low solubility of cellulose in most solvents.

Pure [BMIM]Cl IL system

To calibrate the force field parameters used in our simulations for describing [BMIM]Cl IL, we have calculated the liquid density at 298 K. The theoretical value is 1.075 g cm^{-3}, which is in good agreement with the experimental finding, 1.08 g cm^{-3} [60].

To better understand the property of [BMIM]Cl, we also studied its local structure by analyzing the radial and spatial distribution functions of ions, RDFs and SDFs. Figure 2 shows the calculated RDFs, where $g(r)_{ca}$, $g(r)_{cc}$ and $g(r)_{aa}$ represent the RDF of cation–anion, cation–cation and anion–anion respectively. Obviously, all RDFs show damped oscillations within 2.1 nm which is about half-length of the unit cell, and this coincides with the feature of a strongly coupled ionic system [61]. As seen from Fig. 2, the first peak of $g(r)_{ca}$ locating at about 0.45 nm, is much stronger than those of $g(r)_{cc}$ and $g(r)_{aa}$. This is attributed to the strong electrostatic attraction between cations and anions. The $g(r)_{cc}$ shows a shoulder around 0.4 nm, which may be the result of π–π stacking interactions between imidazolium rings [62]. Furthermore, we found that the minima and maxima positions of $g(r)_{ca}$ coincide with the maxima and minima positions of $g(r)_{cc}$ and $g(r)_{aa}$ with just a little shifts. This feature shows a long-range ordered structure of [BMIM]Cl IL.

The calculated three-dimensional structures of SDFs within 0.7 nm of anions or cations around a cation are given in Fig. 3, where panels (a) and (b) represent the 3D density distribution of anions and cations around the given cation, and panels (c) and (d) are two different views of the superimposed isosurface from panels (a) and (b). We find that the anions are highly directional (panel (a) in Fig. 3), and three large lobes are found to direct roughly along the C2–H, C4–H and C5–H bonds, indicating that the anions lie mainly in the vicinity of these areas. From the isosurface of cations shown in panel (b) in Fig. 3, it is clear that the cations mainly occur in four positions: the areas around C2–H and C5–H bonds, and the areas above and below the imidazolium ring. As shown in panels (c) and (d), we clearly find that anions occupied the first coordination shell of the central cation, and cations appeared in the second shell. The two lobes of cation isosurface along C2–H and C5–H bonds coordinate to anions in the first shell via the electrostatic interaction. And two other lobes above and below the imidazolium ring locate about 0.45 nm from the cation center via the π–π stacking interaction of imidazolium rings, which account for the shoulder around 0.4 nm in $g(r)_{cc}$ in Fig. 2. These features suggest that the anions and cations have formed well-defined ion-pair clusters. All these results of MD simulations for pure [BMIM]Cl IL are in good agreement with experimental data [60] and previous theoretical results [29, 30].

Cellulose oligomer/[BMIM]Cl systems

For three MD equilibrated cellulose oligomer/[BMIM]Cl systems, our attention focuses on the located structures around the oligomers. Figure 4 shows the geometries of three cellulose oligomers with neighboring anions and cations after the MD simulations. It is found that (i) the number of anions around the oligomers is much more than that of cations, and (ii) the anions locate closer distance around the oligomer than the cations. As shown in Fig. 4, chloride anions interact with the oligomer via Cl···H–O

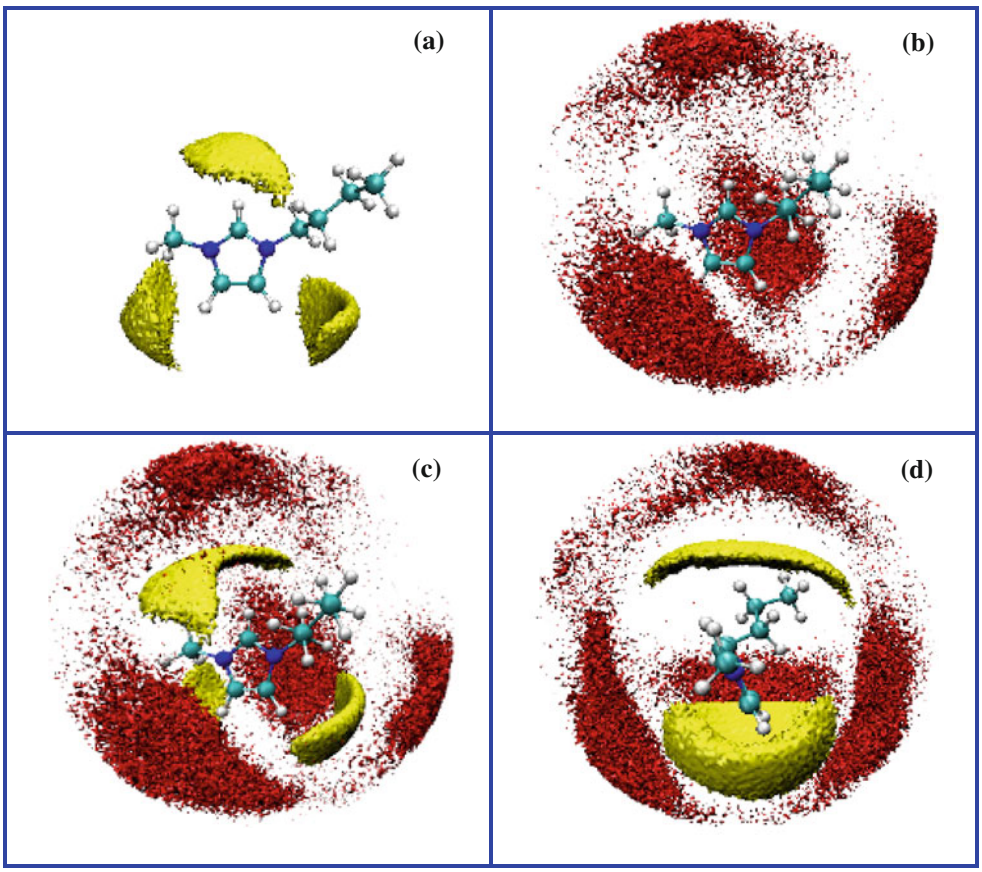

Fig. 3 *Colored* SDFs within 0.7 nm for (**a**) anions around a cation with the *yellow* isosurface, (**b**) cations around a cation with the *red* isosurface, and (**c**) and (**d**) two different views of the superimposed isosurface from (**a**) and (**b**)

hydrogen bonds, whose lengths vary between 1.9 and 2.2 Å; while imidazolium cations link to the oligomer via relatively weak C–H···O hydrogen bonds, as indicated by the calculated larger hydrogen bond lengths ranging from 2.2 to 2.6 Å. All these lengths are shorter than the summations of the van der Waals radii of Cl and H atoms (2.95 Å), and O and H (2.72 Å). The corresponding values of Cl···H–O and C–H···O angles vary ranging from 140 to 180° and from 120 to 160°, respectively. These data confirm the efficient hydrogen bonds between the oligomers and the IL's anions/cations. Furthermore, we also find that upon interaction with the IL, the geometries of cellulose oligomers have changed a lot. The most significant structural information obtained from the present MD simulations for all three systems is that the intramolecular hydrogen bonds in free cellulose oligomers are remarkably destroyed, while the intermolecular hydrogen bonds between the hydroxyl groups in the oligomers and chloride anions/imidazolium cations are formed. For instance, the intramolecular hydrogen bond in the free cellubiose (panel (b) in Fig. 1) with an effective distance of 1.907 Å has been cleaved due to the formation of Cl···H–O and C–H···O hydrogen bonds, as shown in panels (a) and (b) in Fig. 4.

To better understand the distribution of cations/anions around the cellulose oligomer, we also calculated RDFs between cellulose oligomer and anions or cations. Because the oligomers are long-chain molecules, the center-of-geometry RDFs of whole molecules are not suitable for describing the distribution of cations/anions around cellulose oligomer. Thus the hydroxyl groups of oligomers were taken into account to compute the RDFs with cations/anions. As a representative, we show the calculated results of the cellulose oligomer of $n = 2$ with the IL system in Fig. 5, where the RDFs between each of eight hydroxyl groups in cellubiose and anions (panel (a)) or cations (panel (b)) are given in different colors. Similar results for the systems with the oligomers of $n = 4$ and 6 are not given for simplification. In all $g(r)_{\text{O–H···Cl}}$ RDFs, there are sharp peaks at $\sim$0.25 nm, indicating that there are strong interactions between the hydroxyl groups and anions. And in $g(r)_{\text{O–H···BMIM}}$ RDFs, the peaks are located at larger distance (>0.4 nm) and the intensities are much weaker than those of $g(r)_{\text{O–H···Cl}}$ RDFs. These results strongly suggest that anions occupy the first coordination shell around the cellulose oligomer and cations occur outside anions. So chloride anions play a much more important role for the cellulose dissolution than imidazolium cations.

In order to further understand the interaction of the IL with the cellulose oligomer, we furthermore analyzed the hydrogen bond interactions in detail between the oligomer and anions or cations by scanning the trajectory files of the MD simulations. The collected results for the oligomer-IL

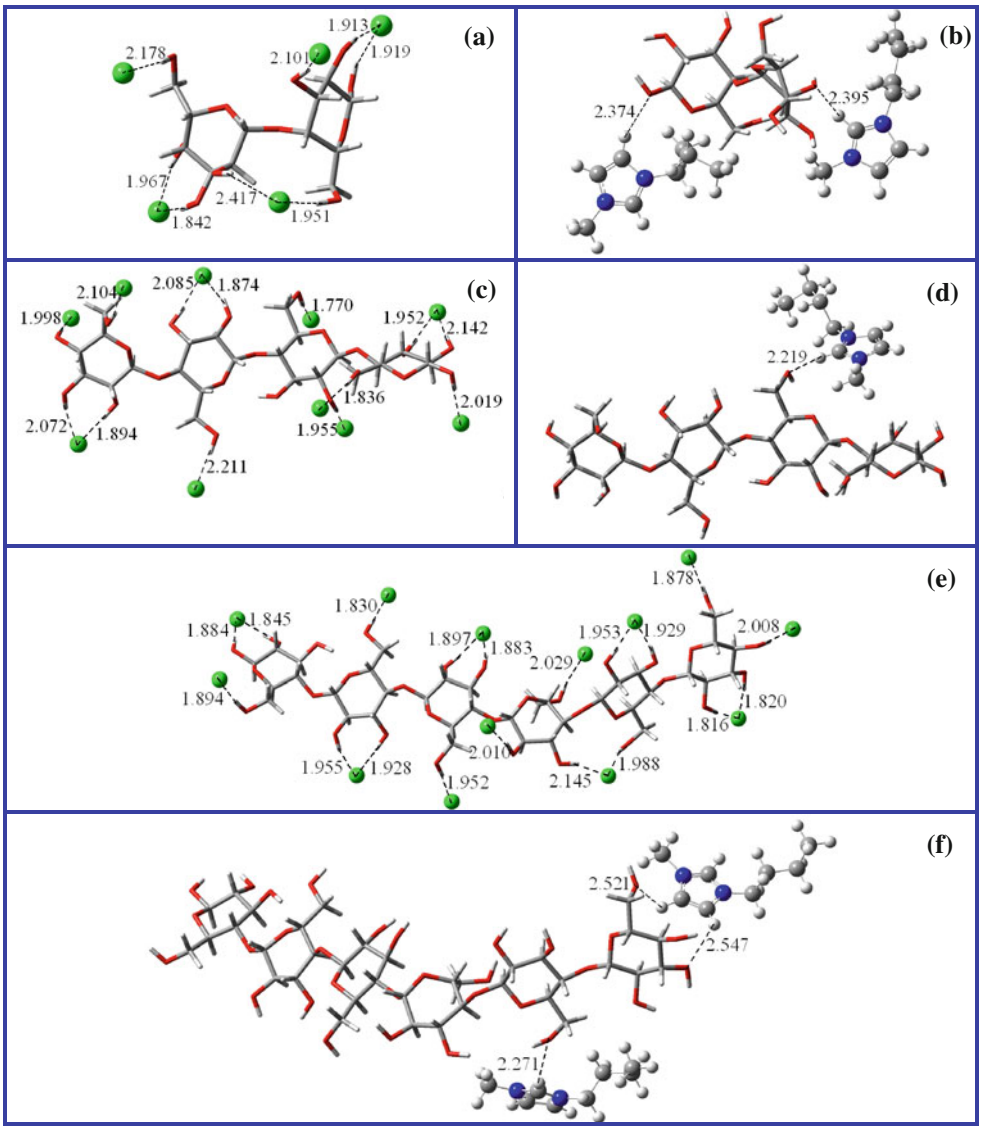

Fig. 4 Structures of three cellulose oligomers with neighboring anions (**a**, **c**, **e**) for $n = 2$, 4, and 6, respectively) and actions (**b**, **d**, **f**) for $n = 2$, 4, and 6, respectively), drawn out from the MD trajectory files

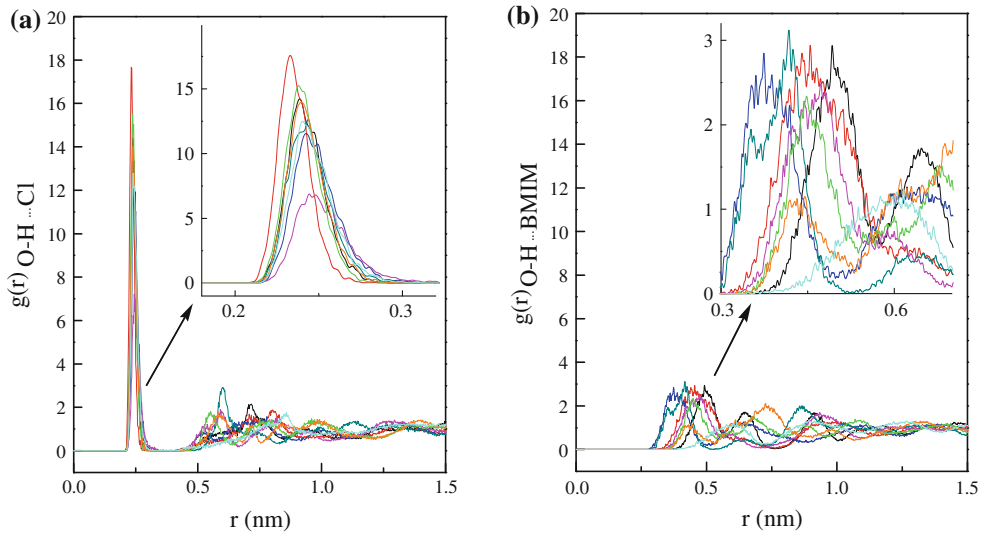

Fig. 5 Calculated RDFs between the hydroxyl groups in the oligomer and anions (**a**) or cations (**b**) of the IL for the oligomer/IL system with $n = 2$. *Insets* show the enlargement of peaks

Table 1 Scanned H-bonds from the oligomer/IL systems after MD simulations[a]

Cellulose oligomers ($n = 2$)/IL system				Cellulose oligomers ($n = 4$)/IL system			
(I)[b] 3.5 Å, 130–180°		(II)[b] 3.3 Å, 150–180°		(I)[b] 3.5 Å, 130–180°		(II)[b] 3.3 Å, 150–180°	
Donor	Acceptor	Donor	Acceptor	Donor	Acceptor	Donor	Acceptor
O1	Cl	O1	Cl	O1	Cl	O1	Cl
O2	Cl	O2	Cl	O2	Cl	O2	Cl
O3	Cl	O3	Cl	O3	Cl	O3	Cl
O6	Cl	O6	Cl	O6	Cl	O6	Cl
O2′	Cl	O3′	Cl	O2′	Cl	O2′	Cl
O3′	Cl	O4′	Cl	O6′	Cl	O6′	Cl
O4′	Cl	O6′	Cl	O2″	Cl	O2″	Cl
O6′	Cl			O3″	Cl	O3″	Cl
C_{BMIM}	O1			O6″	Cl	O6″	Cl
C_{BMIM}	O2′			O2‴	Cl	O2‴	Cl
				O3‴	Cl	O4‴	Cl
				O4‴	Cl	O6‴	Cl
				O6‴	Cl	O3′	O5″
				O3′	O5″		
				C_{BMIM}	O2′		
				C_{BMIM}	O3′		
				C_{BMIM}	O4′		
				C_{BMIM}	O6′		
				C_{BMIM}	O5‴		

[a] Superscripts ′, ″, ‴ represent different glucose rings, and C_{BMIM} represents imidazolium ring carbon atoms. The atom numbering is marked in Fig. 1

[b] The distance and angle denote the scanned H-bond distances (donor–acceptor) and the H-bond angle range (donor–hydrogen–acceptor)

systems with $n = 2$ and 4 are listed in Table 1, where all proton donors and proton acceptors of hydrogen bonds are given for situations (I) and (II). In these two situations, the scanned H-bond distances (donor–acceptor) are within 3.5 and 3.3 Å and the H-bond angle ranges (donor-hydrogen-acceptor) are from 130 to 180° and from 150 to 180°, respectively. We find that chloride anions as proton acceptors generally form effective hydrogen bonds with the oligomer's hydroxyl groups acting as proton donors, and imidazolium cations as proton donors also form hydrogen bonds with the oxygen atoms of the oligomer's hydroxyl groups as proton acceptors. The results for the system with $n = 6$ are exactly similar with the systems with $n = 2$ and 4, so we didn't list the calculated data here for simplification.

The results above clearly indicate that both the anions and cations of the IL can form hydrogen bonds with the hydroxyl groups of cellulose oligomers, however, the strength and number of hydrogen bonds formed by anions are much larger than cations.

To compare the interactions of the oligomer with cations/anions of the IL, we calculated the interaction energies (ΔE) between cellulose oligomer and cations/anions. ΔE is defined as the summation of electrostatic energy (ΔE_{Coul}) and van der Waals interaction energy (ΔE_{LJ}) [63, 64] using Eq. (2):

$$\Delta E = \Delta E_{Coul} + \Delta E_{LJ} \quad (2)$$

Fig. 2S in the electronic supplementary material shows the time evolvement of the interaction energy between the oligomer and anions or cations of the IL. Table 2 lists the calculated mean contributions of Coulomb and Lennard–Jones interactions to ΔE. It is found that the Coulomb interaction is dominant in ΔE_{a-o}, while the van der Waals interaction is primary in ΔE_{c-o}. Furthermore, the mean values of ΔE_{a-o} for three systems with $n = 2$, 4 and 6 are -483.58, -802.76, $-1{,}154.41$ kJ mol^{-1}, which are almost twice greater in absolute value than the corresponding those of ΔE_{c-o}, -204.23, -308.41, -514.32 kJ mol^{-1}, respectively. These results suggest again that the anions play a much more important role than the cations for the dissolution of cellulose in the IL.

Our present results do not support the view of Zhang et al. [34], who speculated that imidazolium cations play a critical role in the cellulose dissolution. However, while emphasizing the critical role of chloride anions in the

Table 2 Mean values of Coulomb and Lennard–Jones interaction energies between the cellulose oligomer and anions or cations

Systems	ΔE_{a-o} (kJ mol^{-1})		ΔE_{c-o} (kJ mol^{-1})	
	ΔE_{Coul}	ΔE_{LJ}	ΔE_{Coul}	ΔE_{LJ}
Cellulose oligomer ($n = 2$)/IL	−574.26	90.68	−39.76	−164.47
Cellulose oligomer ($n = 4$)/IL	−944.41	141.65	−25.60	−282.81
Cellulose oligomer ($n = 6$)/IL	−1374.67	220.26	−76.73	−437.59

cellulose dissolution in [BMIM]Cl, we do not think the interaction of imidazolium cations with cellulose is non-specific, as claimed by Remsing et al. [32, 33]. In contrast, we propose that both chloride anions and imidazolium cations contribute to the cellulose dissolution in [BMIM]Cl, but in different degrees: (i) the anions occupy the first coordination shell around the cellulose oligomer and the cations occur outside anions, (ii) the hydrogen bond distances between anions/cations and the oligomer are in ranges of 1.9–2.2 and 2.2–2.6 Å, respectively, and (iii) the interaction energy of anions with the cellulose oligomer is 2.2–2.6 times of those of cations. These calculated results proposed that chloride anions play a critically important role and imidazolium cations have also present a nonnegligible contribution for the cellulose dissolution in [BMIM]Cl. Our claim is in good agreement with the recent report by Singh et al. [30], who examined the behavior of cellulose oligomers in 1-ethyl-3-methylimidazolium acetate IL by performing MD simulations, and found that cellulose oligomers form strong hydrogen bonds with the acetate anion and are also in close contact with the imidazolium cations.

Conclusions

In summary, we have carried out MD simulations of pure [BMIM]Cl IL and three cellulose oligomer/IL systems to better understand the mechanism of cellulose dissolution in imidazolium chloride ILs at the molecular level. [BMIM]Cl IL is shown to be a strongly coupled system and has a long-range ordering structure with alternative arrange of anions and cations. From the collected data on the oligomer/IL systems, it clearly indicates that both chloride anions and imidazolium cations form hydrogen bonds with the oligomer, whose hydroxyl groups act as the hydrogen bond donors and acceptors, respectively. However, the strength and number of hydrogen bonds and the interaction energy of chloride anions with the oligomer are much larger than that of imidazolium cations, implying that chloride anions of the IL are mainly responsible for the observed effective dissolution of cellulose in the IL, whereas imidazolium cations of the IL play a relatively less important role. Based on the present results, we propose that the cellulose dissolution in [BMIM]Cl IL is a result of the combined interactions of anions and cations with cellulose. The theoretical results show a picture of the dissolution mechanism of cellulose in imidazolium chloride ILs and may offer assistance to develop new and powerful IL-based solvents for dissolution and processing of cellulose.

Acknowledgment We thank the grant from the National Natural Science Foundation of China (No. 20773078) and the Higher Educational Science and Technology Program of Shandong Province (No. J11LB08).

References

1. Himmel ME, Ding SY, Johnson DK, Adney WS, Nimlos MR, Brady JW, Foust TD (2007) Science 315:804–807
2. Ragauskas AJ, Williams CK, Davison BH, Britovsek G, Cairney J, Eckert CA, Frederick WJ Jr, Hallett JP, Leak DJ, Liotta CL, Mielenz JR, Murphy R, Templer R, Tschaplinski T (2006) Science 311:484–489
3. Lynd LR, Laser MS, Bransby D, Dale BE, Davison B, Hamilton R, Himmel M, Keller M, McMillan JD, Sheehan J, Wyman CE (2008) Nat Biotechnol 26:169–172
4. Zaldivar J, Nielsen J, Olsson L (2001) Appl Microbiol Biotechnol 56:17–34
5. Lynd LR, Cushman JH, Nichols RJ, Wyman CE (1991) Science 251:1318–1323
6. Henriksson M, Berglund LA, Isaksson P, Lindström T, Nishino T (2008) Biomacromolecules 9:1579–1585
7. Heinze T, Liebert T (2001) Prog Polym Sci 26:1689–1762
8. Pinkert A, Marsh KN, Pang S, Staiger MP (2009) Chem Rev 109:6712–6728
9. Wu J, Zhang J, Zhang H, He JS, Ren Q, Guo ML (2004) Biomacromolecules 5:266–268
10. Zhu S, Wu Y, Chen Q, Yu Z, Wang C, Jin S, Ding Y, Wu G (2006) Green Chem 8:325–327
11. Endres F, El Abedin SZ (2006) Phys Chem Chem Phys 8:2101–2116
12. Wishart JF, Castner EW Jr (2007) J Phys Chem B 111:4639–4640
13. Rogers RD, Voth GA (2007) Acc Chem Res 40:1077–1078
14. Welton T (1999) Chem Rev 99:2071–2084
15. Chaban VV, Prezhdo OV (2011) Phys Chem Chem Phys 13:19345–19354
16. Chaban VV, Prezhdo OV (2011) J Phys Chem Lett 2:2499–2503
17. Seddon KR (1997) J Chem Technol Biotechnol 68:351–356
18. Chiappe C, Pieraccini DJ (2005) Phys Org Chem 18:275–297
19. Ranke J, Stolte S, Störmann R, Arning J, Jastorff B (2007) Chem Rev 107:2183–2206
20. Sun H, Qiao BF, Zhang DJ, Liu CB (2010) J Phys Chem A 114:3990–3996
21. Kobrak MN (2006) J Chem Phys 125:064502
22. Hogan CJ Jr, de la Mora JF (2009) Phys Chem Chem Phys 11:8079–8090
23. Graenacher C (1934) Cellulose solution. U.S. Patent 1, 943, 176
24. Swatloski RP, Spear SK, Holbrey JD, Rogers RD (2002) J Am Chem Soc 124:4974–4975
25. Guo JX, Zhang DJ, Liu CB (2010) J Theor Comput Chem 9:611–624
26. Guo JX, Zhang DJ, Duan CG, Liu CB (2010) Carbohyd Res 345:2201–2205
27. Youngs TGA, Holbrey JD, Deetlefs M, Nieuwenhuyzen M, Gomes MFC, Hardacre C (2006) Chem Phys Chem 7:2279–2281
28. Youngs TGA, Hardacre C, Holbrey JD (2007) J Phys Chem B 111:13765–13774
29. Liu ZW, Remsing RC, Moore PB, Moyna G (2007) Ion Liq IV Chapter 23:335–350
30. Liu HB, Sale KL, Holmes BM, Simmons BA, Singh S (2010) J Phys Chem B 114:4293–4301
31. Youngs TGA, Holbrey JD, Mullan CL, Norman SE, Lagunas MC, D'Agostino C, Mantle MD, Gladden LF, Bowron DT, Hardacre C (2011) Chem Sci 2:1594–1605
32. Remsing RC, Swatloski RP, Rogers RD, Moyna G (2006) Chem Commun 12:1271–1273
33. Remsing RC, Hernandez G, Swatloski RP, Massefski WW, Rogers RD, Moyna G (2008) J Phys Chem B 112:11071–11078
34. Zhang H, Wu J, Zhang J, He JS (2005) Macromolecules 38:8272–8277

35. Zavrel M, Bross D, Funke M, Büchs J, Spiess AC (2009) Bioresour Technol 9:2580–2587
36. Singh S, Simmons BA, Vogel KP (2009) Biotechnol Bioeng 104:68–75
37. Himmel ME (2008) Biomass recalcitrance. Wiley-Blackwell, London
38. Updegraff DM (1969) Anal Biochem 32:420–424
39. Murakami MA, Kaneko Y, Kadokawa JI (2007) Carbohydr Polym 69:378–381
40. Klemm D, Heublein B, Fink HP, Bohn A (2005) Angew Chem Int Ed 44:3358–3393
41. Woods Group (2005–2011) GLYCAM Web. Complex Carbohydrate Research Center, University of Georgia, Athens, GA. http://www.glycam.com
42. Frisch MJ, Trucks GW, Schlegel HB, Scuseria GE, Robb MA, Cheeseman JR, Montgomery JA Jr, Vreven T, Kudin KN, Burant JC, Millam JM, Iyengar SS, Tomasi J, Barone V, Mennucci B, Cossi M, Scalmani G, Rega N, Petersson GA, Nakatsuji H, Hada M, Ehara M, Toyota K, Fukuda R, Hasegawa J, Ishida M, Nakajima T, Honda Y, Kitao O, Nakai H, Klene M, Li X, Knox JE, Hratchian HP, Cross JB, Bakken V, Adamo C, Jaramillo J, Gomperts R, Stratmann RE, Yazyev O, Austin AJ, Cammi R, Pomelli C, Ochterski JW, Ayala PY, Morokuma K, Voth GA, Salvador P, Dannenberg JJ, Zakrzewski V G, Dapprich S, Daniels AD, Strain MC, Farkas O, Malick DK, Rabuck AD, Raghavachari K, Foresman JB, Ortiz JV, Cui Q, Baboul AG, Clifford S, Cioslowski J, Stefanov BB, Liu G, Liashenko A, Piskorz P, Komaromi I Martin RL, Fox DJ, Keith T, Al-Laham MA, Peng CY, Nanayakkara A, Challacombe M, Gill PMW, Johnson B, Chen W, Wong MW, Gonzalez C, Pople JA (2004) Gaussian 03, Revision D.01; Gaussian, Inc.: Wallingford CT
43. Cornell WD, Cieplak P, Bayly CI, Gould IR, Merz KM, Ferguson DM, Spellmeyer DC, Fox T, Caldwell JW, Kollman PA (1995) J Am Chem Soc 117:5179–5197
44. Liu ZP, Huang SP, Wang WC (2004) J Phys Chem B 108:12978–12989
45. Chaban VV, Voroshylova IV, Kalugin ON (2011) Phys Chem Chem Phys 13:7910–7920
46. Chaban V (2011) Phys Chem Chem Phys 13:16055–16062
47. Chaban VV, Voroshylova IV, Kalugin ON (2011) ECS Trans 33:43–55
48. Kirschner KN, Yongye AB, Tschampel SM, Daniels CR, Foley BL, Woods RJ (2008) J Comput Chem 29:622–655
49. Berendsen HJC, van der Spoel D, van Drunen R (1995) Comput Phys Commun 91:43–56
50. van der Spoel D, Lindahl E, Hess B, Groenhof G, Mark AE, Berendsen HJC (2005) J Comp Chem 26:1701–1718
51. Hess B, Kutzner C, van der Spoel D, Lindahl E (2008) J Chem Theory Comp 4:435–447
52. Lindahl E, Hess B, van der Spoel D (2001) J Mol Mod 8:306–317
53. Darden T, York D, Pedersen L (1993) J Chem Phys 98:10089–10092
54. Essmann U, Perera L, Berkowitz ML, Darden T, Lee H, Pedersen LG (1995) J Chem Phys 103:8577–8593
55. Berendsen HJC, Postma JPM, van Gunsteren WF, DiNola A, Haak JR (1984) J Chem Phys 81:3684–3690
56. Bondi A (1964) J Phys Chem 68:441–451
57. Fredlake CP, Crosthwaite JM, Hert DG, Aki SNVK, Brennecke JF (2004) J Chem Eng Data 49:954–964
58. Cowling EB, Kirk TK (1976) Biotechnol Bioeng Symp 6:95–123
59. Reese ET, Mandels M, Weiss AH (1972) Adv Biochem Eng 2:181–200
60. Huddleston JG, Visser AE, Reichert WM, Willauer HD, Broker GA, Rogers RD (2001) Green Chem 3:156–164
61. Keblinski P, Eggebrecht J, Wolf D, Phillpot SR (2000) J Chem Phys 113:282–291
62. Dupont J (2004) J Braz Chem Soc 15:341–350
63. Lv YQ, Lin ZX, Tan TW, Feng W, Qin PY, Li C (2008) Sens Actuators B 133:15–23
64. Zhang HY, Feng W, Li C, Tan TW (2010) J Phys Chem B 114:4876–4883